AUTOMATED VERIFICATION OF ROAD NETWORK DATA BY VHR SATELLITE IMAGES USING ROAD STATISTICS

W.Goeman, L.Martinez-Fonte, R.Bellens, S.Gautama

Dept. Telecommunication and Information Processing, Ghent University
St.Pietersnieuwstraat 41, B-9000 Gent, Belgium
wgoeman@telin.ugent.be
Ghent University

KEY WORDS: Quality assessment, ridge detection, performance characterization, road extraction, spatial accuracy, GIS

ABSTRACT:

A method is explored to assess the quality of road network data based on image information in a reliable and accurate way. Therefore, the quality of the image information resulting from a ridge extraction procedure is characterized in terms of detection rate. The optimal parameter set for the ridge extraction is predicted based on typical road samples extracted from the image, resulting in an optimal performance of the road detection. In the field of geography, an accuracy assessment method, called buffer-overlay-statistics, is known to assess the spatial quality of a line data set by using another line data set of higher spatial accuracy. Here, the method is adapted to assess the quality of a line data set based on image information rather than vector data. The average displacement accuracy measure is redefined, such that it is able to take into account line detection errors (fragmentation and noise). Experiments were conducted on IKONOS panchromatic and Quickbird multispectral satellite images.

1. INTRODUCTION

Within the field of geographic information systems, a major challenge is the continuous assessment and control of the quality of the spatial data. The rapid growing number of sources of geospatial data, ranging from high-resolution satellite and airborne sensors, GPS, and derivative geospatial products, poses severe problems for integrating data. This can be especially difficult in an urban or suburban context, where the density and variety of observed structures is very high.

Content providers face the problem of continuously ensuring that the information they produce is reliable, accurate and up-to-date. Integrity constraints are able to resolve certain issues in the data, like valid attribute values or relationships between data objects. The main issue is however the consistency of the data with respect to the current "real-world" situation. Part of this problem is handled using image interpretation from aerial photos and very-high-resolution satellite images. Although this is still mainly a manual process performed by human operators, automated detection of change and anomalies in the existing databases using image information can form an essential tool to support quality control and maintenance of spatial information.

There are several standards for spatial data quality at the national, regional and international levels (FGDC, 1995; ASPRS, 1990; ISO, 1999). In view of that, components of the quality of spatial data are defined, which include positional accuracy, attribute accuracy, logical consistency, completeness, and lineage. Since the positional accuracy component and the completeness are the most related components to this study, the other three components of the spatial data quality are introduced shortly first. Attribute accuracy, the second component of quality of spatial data addresses the quality of the characteristics of spatial data and how well that matches reality. Logical consistency is defined as the fidelity of relationships described by the data structure. The lineage of a database includes reference to source materials, data collection procedures, and pre-processing including geometric transformations applied to the spatial data. Completeness refers to mapping rules applied in equal way to all data and is sometimes referred to as exhaustiveness. It identifies gaps in the data progression and indicates whether missing values have been encountered.

The Spatial Data Transfer Standard (SDTS) identifies four methods for assessing the positional accuracy of a digital dataset. These include deductive estimate, internal evidence, comparison to source and comparison to independent source of higher accuracy. Deductive estimate is the practical estimate of errors in the source of spatial data including the assumptions made about error propagation. Internal evidence refers to all possible statistics or adjustments that may be used on the spatial data. Comparison to the source means comparing the derived spatial data with the original source. Among these spatial data quality standards, it is noticed that they all pointed out that comparison to an independent source of higher accuracy is the preferred method for assessing positional accuracy of a digital dataset (USGS, 1999).

While standard practice still relies on comparing control points, current applications put stricter demands on shape fidelity and relative accuracy. This means that the positional and the geometrical quality of their representations should not depend only on the individual points, which are part of its representation, but on the interrelationships and precise portrait of all these points. In the literature, there is little published on how one can verify the shape of a linear data set (e.g. a road network data set) by another set (of higher accuracy). Ramirez (2000) introduced four positional quality measures to express the similarity between two line presentations: the generalization factor, the distortion factor, the bias factor and the fuzziness factor.   The first three quality measures basically use the segment lengths measured along the two corresponding line representations to express in some way their resemblance. The last measure uses only the end points of the two line representations.   Another approach for the assessment of positional quality of linear features of particular interest can be found in (Goodchild and Hunter, 1997) and (Tveite and Langaas, 1999).   The two approaches use a buffer overlay concept. The two lines both get a buffer at distance r. By comparing the area of the different zones, one is able to calculate the average displacement, the oscillation of the lines and an indication of the spatial bias. These quality measures are

based on statistics, relatively insensitive to outliers and do not

require matching of points between representations.

**Figure 1: Left: Ridge detection result in satellite image.
Right: Corresponding road vector data**

However, the main question that is addressed here, is how a system for quality assessment can make optimal use of image derived information, which inherently is inaccurate and incomplete. The quality measures in the literature are devised to compare vector data and do not take into account the errors that can occur in image derived information. In our work, we explore what statements can be made to compare image and vector information. Because it is difficult to guarantee consistent quality of image information on an object level, we focus on making reliable statements on a region level.

By characterizing the properties of regions, quality can be described in a statistical sense instead of using a comparison of individual objects. While this somehow relaxes the demand for a complete image description, it still remains vital to characterize the detection in terms of accuracy and completeness. Fig. 1 shows a comparison between image and vector information. Shadow, occlusion and variety in appearance all give rise to a fragmented and imprecise description of the image content. For a statistic like BOS to make sense, the performance of the detection needs to be quantified (i.e. spatial accuracy, number of false segments, mean true and false segment length). Without such a performance characterization it becomes difficult to map the reliability of quality measures.

In next section, we describe the ridge extraction for road detection. Section 3 gives details on the methodology for characterizing the performance based on error propagation. Section 4 deals with the quality assessment of road vector data, based on image information. Section 5 shows experimental results performed on very-high-resolution satellite images. Section 6 concludes the paper with a brief discussion.

2. RIDGE DETECTION

If we look at the intensity image as a terrain model, lines can be identified as narrow valleys in the intensity image. In (Steger, 1998), different approaches to line detection are reviewed. In this work, line detection is performed based on polynomial interpolation to determine pixels belonging to road structures in the image, the "facet model" (Haralick, 1983). This is a standard method for ridge detection. The image is regarded as a function I(i, j). Lines are detected as ridges and ravines in this function by locally approximating the image function by its second order Taylor polynomial. The polynomial is used to approximate first and second order derivatives of the image function in each pixel. The direction of the line can be determined from the Hessian matrix of the Taylor polynomial.

The gradient and curvature information in each pixel are used to classify a pixel in a number of topological classes based on their sign or magnitude. Line points are mainly characterized by a high second directional derivative, i.e. a high curvature perpendicular to the line direction. The calculation of the partial derivatives can be done in various ways. The facet model determines a least squares fit of a polynomial F to the image data I over a window of size $N = w^2$ with window size w. The origin is chosen in the central pixel of the window. The value of the polynomial F in pixel (i, j) is given by:

$$F(i, j, \boldsymbol{\theta}) = a_1 + a_2 i + a_3 j + a_4 i^2 + a_5 ij + a_6 j^2$$
$$= \mathbf{m}^T \boldsymbol{\theta} \tag{1}$$

$$with \quad \mathbf{m} = \begin{bmatrix} 1 & i & j & i^2 & ij & j^2 \end{bmatrix}^T$$
$$\boldsymbol{\theta} = \begin{bmatrix} a_1 & a_2 & a_3 & a_4 & a_5 & a_6 \end{bmatrix}^T$$

The facet model searches the least-squares solution $\boldsymbol{\theta}$, given the image data $\mathbf{x}$ containing the intensity value I(i, j) in each pixel (i, j):

$$\underset{\boldsymbol{\theta}}{\arg\min} \, r(\boldsymbol{\theta}) \quad with \quad r(\boldsymbol{\theta}) = \left\| \mathbf{M}\boldsymbol{\theta} - \mathbf{x} \right\|^2 \tag{2}$$

$$M = \begin{bmatrix} 1 & i_1 & j_1 & i_1^2 & i_1 j_1 & j_1^2 \\ . & . & . & . & . & . \\ 1 & i_N & j_N & i_N^2 & i_N j_N & j_N^2 \end{bmatrix}^T \in \Re^{Nx6}$$

$$\mathbf{x} = \begin{bmatrix} I(i_1, j_1) & ... & I(i_N, j_N) \end{bmatrix}^T \in \Re^{Nx1}$$

This leads to the linear system $M^T M \boldsymbol{\theta} = M^T \boldsymbol{x}$ with the solution $\boldsymbol{\theta_0}$ given by $\boldsymbol{\theta_0} = (M^T M)^{-1} M^T \boldsymbol{x}$. The matrix M is independent of the position of the window within the image, meaning that the calculation of $(M^T M)^{-1} M^T$ needs to be performed only once for the processing of an image with a fixed window size w. On the basis of the parameters $\boldsymbol{\theta}$ of the interpolated surface F, the gradient and Hessian in a certain pixel can be calculated. In our model we are only interested in the gradient and the Hessian in the central pixel of the window (i.e. i=j=0)

$$gradient(I) = \begin{bmatrix} \dfrac{\partial I}{\partial x} & \dfrac{\partial I}{\partial y} \end{bmatrix}^T = \begin{bmatrix} a_2 + 2a_4 i + a_5 j \\ a_3 + a_5 i + 2a_6 j \end{bmatrix}$$

$$Hessian(I) = \begin{bmatrix} \dfrac{\partial^2 I}{\partial x^2} & \dfrac{\partial^2 I}{\partial x \partial y} \\ \dfrac{\partial^2 I}{\partial x \partial y} & \dfrac{\partial^2 I}{\partial y^2} \end{bmatrix} = \begin{bmatrix} 2a_4 & a_5 \\ a_5 & 2a_6 \end{bmatrix} \tag{3}$$

3. ERROR ANALYSIS

We wish to give a more quantitative analysis of the performance of ridge detection. More specifically, we wish to be able to predict the performance of the detector for a given dataset and the according parameter set that gives optimal results. For this, we analyze the influence that perturbations on the intensity values have on the estimation of the parameters by using error propagation (Haralick, 1996). Additive random perturbations

are assumed on the input $\mathbf{x}$ and the perturbations are described by the covariance matrix $\mathbf{\Sigma_x}$. The propagation of the error on the input $\mathbf{x}$ to the estimated parameters $\mathbf{\theta}$ is given by:

$$\mathbf{x} = \mathbf{x} + \Delta\mathbf{x}, \mathbf{\theta} = \mathbf{\theta} + \Delta\mathbf{\theta},$$

$$\Sigma_{\Delta\theta} = (M^T M)^{-1} M^T \Sigma_{\Delta x} M (M^T M)^{-1} \quad (4)$$

The matrix $(M^T M)^{-1} M^T$ can be worked out to a closed expression. Due to the linear system, the error propagation of x on θ is only dependent on the window size w and not on the input intensity values (and consequently independent of the observed perturbed image structure). For uncorrelated noise with variance σ^2, Eq.(4) simplifies to $\Sigma_{\Delta\theta} = \sigma^2(M^T M)^{-1}$ since in this case $\Sigma_{\Delta x} = \sigma^2 I$. However, in this work, the general case is followed.

The parameter covariance matrix $\Sigma_{\Delta\theta}$ allows estimating the variance on the detected gradient and curvature of the ridge detector. The gradient magnitude and eigenvalues of the Hessian are given by:

$$G \equiv \|\mathbf{g}\| = \sqrt{a_2^2 + a_3^2}$$

$$\lambda_{1,2} = a_4 + a_6 \pm \sqrt{a_4^2 + a_5^2 + a_6^2 - 2a_4 a_6} \quad (5)$$

The variance on these measurements up to the first order is given by

$$\sigma_G^2 = \left(\frac{\partial G}{\partial\theta}\right)^T \Sigma_\theta \left(\frac{\partial G}{\partial\theta}\right)$$

$$\sigma_{\lambda_1}^2 = \left(\frac{\partial\lambda_1}{\partial\theta}\right)^T \Sigma_\theta \left(\frac{\partial\lambda_1}{\partial\theta}\right) \quad (6)$$

In combination with Eq.(4), this gives the relation between the perturbations on the image data and the perturbations on the detection measurements G and λ_1. This relation allows estimating the expected performance of the detector for a given parameter set in terms of detection rate. The basic ridge detector operates by setting a threshold t_1 on the first eigenvalue λ_1 of the Hessian. Pixels that exceed this threshold are selected as ridge pixels. To predict the performance of the detector, the eigenvalue λ_1 is regarded as a stochastic variable using a Gaussian distribution with variance σ_{λ_1}. The probability $p(\lambda_1 > t_1)$ expresses when the curvature λ_1 of a pixel exceeds t_1. This distribution is given by the survival function (i.e. the complement of the cumulative density function) of the Gaussian:

$$p(\lambda_1 > t_1) = \frac{1}{\sigma_{\lambda_1}\sqrt{2\pi}} \int_{t_1}^{\infty} e^{-\frac{(\lambda_1 - \overline{\lambda_1})^2}{2\sigma_{\lambda_1}^2}} d\lambda_1$$

$$= \frac{1}{2}\left[1 - erf\left(\frac{\lambda_1 - \overline{\lambda_1}}{\sigma_{\lambda_1}\sqrt{2}}\right)\right] \quad (7)$$

Given the survival function, calculated with the appropriate statistics for the road, a prediction of the detection performance can be made in terms of true positive and false negative detection. In addition, if statistics for the noise structures in the surroundings of a road (e.g. buildings, trees) are measured, a prediction of the false positive and true negative detection can be made.

4. QUALITY ASSESSMENT

When digitizing features, one always introduces uncertainty on the spatial accuracy of the digitized representation because of problems with measuring methods, frames of geodetic reference and feature definitions. In order to assess the positional accuracy of a feature's digital representation, one can compare it's location with one derived from a source with higher accuracy. It is assumed that the accuracy of the reference source is sufficiently high, such that the difference between it and the truth can be ignored. The comparison results in some quality metrics, which are property of the tested source only. Here, we focus on the quantification of the geometric accuracy of lines. Based on the definition given by the vector based buffer-overlay-statistics (BOS) method, a displacement accuracy measure will be defined expressing the deviation of the road vector data from the road information extracted out of a satellite image.
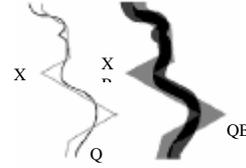

Figure 2: The buffer overlay statistics method

4.1 Buffer-overlay-statistics method

The method uses two independent line data sets, X and Q, representing the road vector data of the same roads in the same area. The geometric accuracy of Q should be better than the expected geometric accuracy of the vector data X. This method, described in (Goodchild and Hunter, 1997) and (Tveite and Langaas, 1999) use a buffer overlay concept to compare the two data sets. It differs from other methods, such as (Ramirez, 2000), in that it is based on statistics and doesn't need a correspondence between the two linear representations. In this method, the two lines both get a buffer at distance r, see Fig 2. By comparing the area of the different zones (e.g. inside both QB and XB,), one is able to assess the average displacement, the oscillation of the lines and to calculate an indication of the spatial bias.
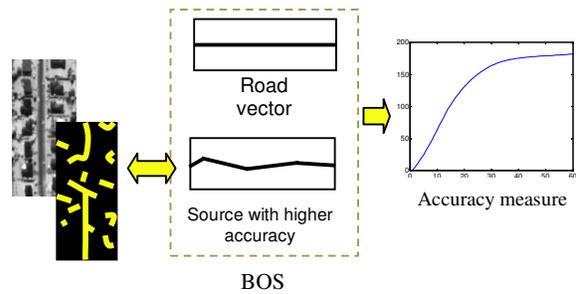

Figure 3. Vector based BOS becomes Image based BOS

$$AvgDisplacement(X) = \pi.b.\frac{area(\overline{XB}\ inside\ QB)}{area(XB)} \quad (8)$$

Fig. 3 shows how the iterative BOS method is applied. To construct the graph on the right, the average displacement is calculated for each buffer size around the vector data X and Q, according to the equation Eq. (8). The graph must be expected to increase steadily with increasing buffer size until it reaches the average displacement of the line data set, then the graph should start to flatten out. The shape of the graph therefore gives an indication of the average displacement.

There are a few remarks to this approach. First, the results are reported in the form of a table or graph, which is difficult to interpret or to handle because there is no quantitative expression of the quality available which could be used in further decision making. Next, the buffer overlay technique requires a complete representation of the linear features in both data sets. Here, a quality assessment of road vector data is performed using image information, which is the result of a ridge extraction procedure, containing a certain degree of fragmentation. Next to this fragmentation, noise will be present and should be, together with the fragmentation, accounted for when constructing the quality measures. In Fig 4, we see an example of such a road extraction result, which will be used as the reference source. But instead of one line with higher accuracy, we have a fragmented line and noise structures due to imperfect road extraction.
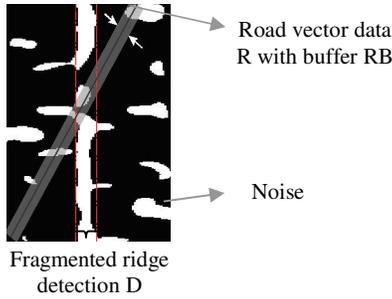

Road vector data R with buffer RB

Noise

Fragmented ridge detection D

Figure 4: Ridge extraction result and buffered vector data in overlay

Due to this fragmentation and noise, the same process cannot be used anymore for assessing the average displacement. In Eq. (8), the noise adds to the value of QB resulting in a bad assessment of the average displacement.

4.2 New approach

Based on previous remarks, we propose a new quality measure which takes into account these shortcomings. Our goal is to construct a measure which indicates how much the road location described by the vector data deviates from the 'real world' situation which is represented by the image information. Fig. 4 shows us a ridge extraction result used as reference source to verify the road vector data.

The method is an iterative process with increasing buffer size, consisting out of the following steps:

- Create a buffer RB of size r around the road vector R.
- Calculate the overlap area O between the buffered vector data RB and the road detection data D.
- Subtract the previous (smaller) buffer size overlap area from O

- Normalize the result by dividing this difference by the increase in area of the buffer RB

This procedure translates in the normalized differential overlap area $F(r)$:

$$F(r) = \frac{area(D \cap RB)_{B=r} - area(D \cap RB)_{B=r-1}}{area(RB)_{B=r} - area(RB)_{B=r-1}} \quad (9)$$

A result of this calculation is given in Fig 5. To interpret this figure, we make a prediction of the expected noise level and detection rate based on a typical road sample, see 5.1. We can now distinguish three regions in the figure:

- The upper region from one to the predicted signal level: due to incompleteness of the ridge detection the graph $F(r)$ will never rise above the predicted signal level.

- The middle region from the maximum signal level to the predicted noise level: a fraction of the value of $F(r)$ is a result from overlap with road signal

- The lower region under the noise level: from this threshold we cannot know whether the value of $F(r)$ is due to noise or to road signal, and must be disregarded.

The dark line represents the ideal case of a road vector perfectly corresponding to the middle of the road in the image. For all buffer sizes smaller than the width of the road in the image, the normalized differential overlap area $F(r)$ is expected to be the predicted detection performance. When the buffer exceeds the road width, $F(r)$ will fall back to the predicted noise level. The graph in light gray shows the case of a small shift between the location of the road in the test source and the reference source. The graph will now be characterized by some intervals located above the noise level, which indicates overlap with road signal at a distance r. This distance will be an underestimation of the true distance because only the shortest path between the two road representations is considered using these buffers.
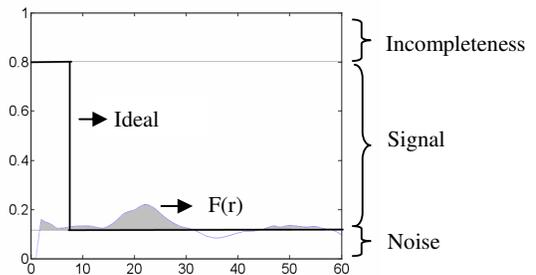

Figure 5: F(r) in relation to the buffer size. Black: Ideal case. Gray: Typical example

Based on this interpretation of the figure, we define the average displacement of the road vector data as the average buffer length of the gray filled region in Fig 5, which translates to:

$$AvgDisplacement = \frac{\int F'(r).r dr}{\int F'(r) dr},$$

(10)

$$F'(r) = \begin{cases} F(r) - \text{NoiseLevel}, & F(r) > \text{Noise Level} \\ 0, & F(r) <= \text{Noise Level} \end{cases}$$

5. EXPERIMENTS

To test the method in practice, we apply the expressions derived in the previous sections. First we'll take a look at the performance of the road extraction then the optimal performance will be derived, and finally a quality assessment of the linear spatial data set is conducted using the adapted BOS. The experiments presented here, were conducted on zones of an IKONOS panchromatic and a Quickbird multispectral satellite image, displaying the city of Ghent, Belgium. A number of small image subsets have been selected containing straight examples of typical roads. These subsets have been manually rotated until each road is positioned parallel to the vertical axis. Fig. 6 shows the selected image subsets referenced R_1 to R_5.
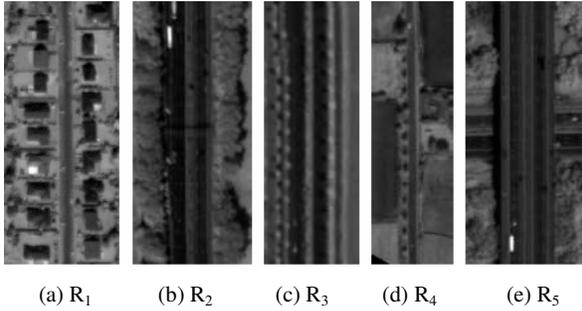

(a) R$_1$　　(b) R$_2$　　(c) R$_3$　　(d) R$_4$　　(e) R$_5$

Figure 6: Road data subset

5.1 Performance characterization

The position x_{road} of the central axis of the road is used to measure the covariance matrix Σ_x and the mean curvature $E[\lambda_1]$, by sampling x and λ_1 for a given window size w. Using Eq. (7) we can make a prediction of the expected detection rate for that type of road. This equation gives rise to a distribution that only gives information about the useful signal, i.e. the road that needs to be detected. This gives an upper bound to the threshold t_1. A lower bound is defined by the properties of the noise, i.e. undesired structures in the image which are falsely detected. If the threshold is chosen too low, the detection of these false negatives will increase. The performance of the detection for each threshold can be summarized in a Receiver Operating Characteristic (ROC) curve. Sensitivity and specificity are defined as follows:

$$\text{sensitivity} = \frac{TP}{TP + FP} = \frac{\text{detected road pixels}}{\text{road length}}$$

$$\text{specificity} = \frac{TN}{TP + FP} = 1 - \frac{\text{detected noise pixels}}{\text{noise length}}$$

(11)

where *{TP, TN,FN, FP}* stands for true positive etc. True positives and false negatives are measured on the road where x is $x = x_{road}$ and are normalized using the total road length in the image. True negatives and false positives are measured along a vertical axis $x = x_{noise}$ representative for the noisy structures in the vicinity of the road. The position of this axis is determined automatically by taking the position of the second largest peak in the mean curvature profile of the road and its vicinity. Normalisation is performed using the total length of the axis, which in this case equals the total road length. Fig. 9a illustrates the position $x = x_{road}$ and $x = x_{noise}$ for road type R_1. The reason for this approach is that it can be meaningful to characterize false detections in the direct surroundings of a road. Since for some applications a rough registration between image and GIS data is known, regions-of-interest can be defined where roads are expected in the image. Road detection in this case should then be aimed at distinguishing the useful signal from noise in the immediate surroundings. In our example we measure the noise statistics of the structures beside the road and use this to model the expected falsely detected noise pixels using Eq.(7). In this case Σ_x and $E[\lambda_1]$ are measured for $x = x_{noise}$ for the same window size w as the signal. Using the ROC curve, the optimal performance for this curve is defined as the point on the curve closest to the upper right corner (1, 1). The upper right corner is equivalent to a road which is completely detected with no detection of noisy structures (i.e. perfect detection). The point on the curve closest to perfect detection defines the optimal threshold t_1 for the given window size. In Fig. 7, the empirical and predicted ROC curves for road type R_1 are plotted for window size $w = 11$ and $w = 13$. The full curve shows the empirical plot, where detected and falsely detected road pixels have been measured on the road axis and the position x_{noise}. The dashed curve shows the predicted plot using the covariance matrices measured in these positions. The sample point closest to the upper right corner defines the optimal threshold for each window size. The difference between the empirical and predicted ROC curve for a given window size is mainly due to a less accurate estimation of the true noise survival function.
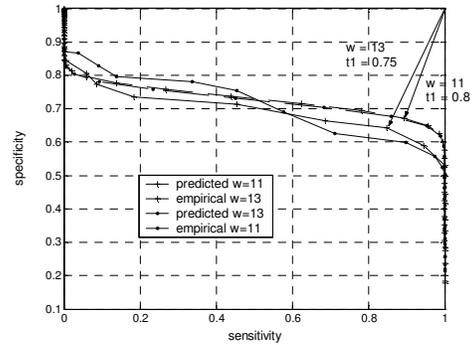

Figure 7: Empirical and predicted ROC curves for road type R1 for window size w = 11 and w = 13. The empirical and predicted point of optimal performance are marked by the arrows.

5.2 GIS quality assessment

To test the image based displacement quality measure, we applied the proposed methodology to a Quickbird test zone, displaying a suburban part of Ghent, shown in Fig. 1. The results of the new (image-based) displacement measure are

compared to the results of the vector based displacement measure in the following way:

- A road network database R is manually plotted over the image, which defines our ground truth with high spatial accuracy.
- A typical road sample is used to predict the road extraction performance for a certain parameter set of the ridge detection.
- The road network database R is shifted D pixels in a chosen direction. This results in a shifted database S.
- We calculate the average displacement D_1 as defined by Tveite and Langaas, using the two vector databases R and S.
- We calculate the average displacement D_2 as described in previous section, using the image information and the vector database S.
- The same procedure is repeated several times with increasing D.

In Fig. 8, we see the result of the calculations of D_1 and D_2 for a shift going from 0 to 120m. The image based method seems to give a good approximation of the corresponding vector based displacement. Although for small shifts, we see a clear overestimation due to the thickness of the detected roads. The method was applied to image information resulting from ridge detection with different parameter settings. From Fig. 8, we conclude that the image based displacement measure doesn't depend much from the detection parameters for road extraction.
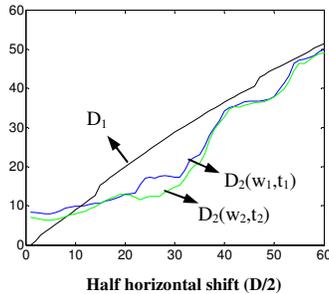

Figure 8: D_1 compared to D_2 for two different parameter settings

It is clear that some shortcomings of the vector based BOS will remain in the image based method. Hence, there is always an underestimation of the displacement compared to the true displacement. The underestimation can be explained by considering a shift of the vector data along the direction of the corresponding road in the image. In that case no mentionable displacement will be detected using buffer overlay statistics. Finally, only the shortest distance between road vector data and image data is considered using this technique. Both factors result in an underestimation of the actual shift.

6. CONCLUSION

Whereas in other research the main focus is on data production, in this paper we focus on how image information can be used to assess the quality of an already existing road vector data base. In the literature, only few techniques are presented to verify a linear vector data set by comparing with another. Using buffer overlay statistics, we can make some quality statements about the tested road vector data without the need of finding an exact correspondence between the tested source and the reference source. But the need for a complete representation of the road vector data is a disadvantage when using image information,

because the ridge detection result is inherently bound to fragmentation and miscoding. Therefore, we propose a framework which sets up the optimal parameters for the ridge detection and makes a prediction about the fragmentation and the noise in the detection result. Based on these predictions, a displacement quality measure is defined which quantitatively expresses the displacement of the tested source compared to the image source.
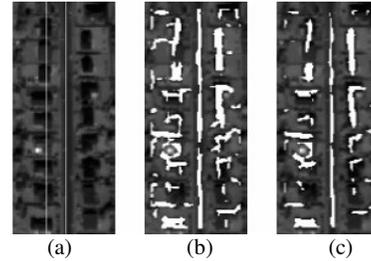

(a) (b) (c)

Figure 9: Detected result on road type R1 using optimal parameter settings. The original image shows the position x = x_{road} and x = x_{noise}. (a) original (b) predicted (c) empirical

7. REFERENCES

References from Journals:
Goodchild F.M. and Hunter J. Gary, A simple positional accuracy measure for linear features.

Haralick, R., 1983, Watson, L. and Laffey, T., The topographic primal sketch, International Journal of Robotics Research 2(1):50–72.

Haralick, R., 1996, Propagating Covariance in Computer Vision, International Journal on Pattern Recognition and Artificial Intelligence 10(5):561–572

Ramirez, J. 2000, Quality Evaluation of Linear Features, A white paper submitted to NIMA.

Steger, C., 1998, An unbiased detector of curvilinear structures, IEEE Transactions on Pattern Analysis Machine Intelligence 20(2):113–125.

References from Other Literature:
American Society for Photogrammetry and Remote Sensing (ASPRS) 1990, Accuracy Standards for Large-Scale Maps, Photogrammetric Engineering and Remote Sensing, 56 (7), pp. 1068-1070.

Federal Geographic Data Committee (FGDC) 1995, *Content Standards for Digital Geospatial Metadata Workbook*, USA.

Federal Geographic Data Committee (FGDC) 1998, A common set of terminology and definitions for the documentation of digital geo-spatial data, *Content Standard for Digital Geo-spatial Metadata (CSDGM),* USA.

International Standard Organization (ISO) 1999, ISO-15046: Geographic Information, Part 13: Quality principles, ISO/TC 211, Doc. No. 478.

References from websites:
United States Geological Survey (USGS) 1999, National Map Accuracy Standards Fact Sheet FS-171-99, http://rockyweb.cr.usgs.gov/nmpstds/nmas.html (09/15/00).